JOURNAL OF THE ROYAL SOCIETY Interface

Sinking velocities of phytoplankton measured on a stable density gradient by laser scanning

Anthony E Walsby and Daryl P Holland

J. R. Soc. Interface 2006 **3**, 429-439
doi: 10.1098/rsif.2005.0106

JOURNAL OF THE ROYAL SOCIETY Interface

J. R. Soc. Interface (2006) **3**, 429–439
doi:10.1098/rsif.2005.0106
Published online 14 December 2005

Sinking velocities of phytoplankton measured on a stable density gradient by laser scanning

Anthony E. Walsby* and Daryl P. Holland

School of Biological Sciences, University of Bristol, Bristol BS8 1UG, UK

Two particular difficulties in measuring the sinking velocities of phytoplankton cells are preventing convection within the sedimenting medium and determining the changing depth of the cells. These problems are overcome by using a density-stabilized sedimentation column scanned by a laser. For freshwater species, a suspension of phytoplankton is layered over a vertical density gradient of Percoll solution; as the cells sink down the column their relative concentration is measured by the forward scattering of light from a laser beam that repeatedly scans up and down the column. The Percoll gradient stabilizes the column, preventing vertical mixing by convection, radiation or perturbation of density by the descending cells. Measurements were made on suspensions of 15 μm polystyrene microspheres with a density of 1050 kg m^{-3}; the mean velocity was 6.28 μm s^{-1}, within 1.5% of that calculated by the Stokes equation, 6.36 μm s^{-1}. Measurements made on the filamentous cyanobacterium *Planktothrix rubescens* gave mean velocities within the theoretical range of values based on the range of size, shape, orientation and density of the particles in a modified Stokes equation. Measurements on marine phytoplankton may require density gradients prepared with other substances.

Keywords: phytoplankton sinking; sedimentation column; Percoll gradient; cyanobacteria; *Planktothrix rubescens*

1. INTRODUCTION

Phytoplankton cells, owing to their small size, sink very slowly through water and this poses technical problems in measuring their sinking velocities. We report here an automated method of measuring sinking velocities by repeatedly scanning a density-stabilized sedimentation column with a laser beam; the method gives results that show good agreement with theoretical values.

Knowledge of sinking velocities explains how phytoplankton remain suspended or show vertical migration in natural waters. Although there is a well-developed theory for objects of simple shape, direct measurements are needed for cells of complex shape, some of which are adaptations that delay sedimentation (Conway & Trainor 1972; Walsby & Xypolyta 1977). Measurements are also needed to investigate apparent anomalies in sinking velocity, such as the changes that occur when cells become senescent or die (Smayda 1971, 1974; Wiseman & Reynolds 1981).

The methods of measuring phytoplankton sinking rates with sedimentation columns were reviewed by Smayda (1970) and Walsby & Reynolds (1981). They fall into two classes, I, mixed, and II, layered.

In class I, the cell suspension is uniformly mixed in a vertical column and the cells left to settle; the sinking velocity is determined from the disappearance of cells from the top section or their arrival at the bottom. Bienfang (1981*a*) recorded the arrival of ^{14}C-labelled cells with a Geiger counter at the base of a sedimentation column. He also developed the 'SETCOL' method in which cells were collected in the bottom compartment of a settling column after a given time (Bienfang 1981*b*); the method is suitable for studies at sea (e.g. Waite & Nodder 2001). A limitation of the method is that the arrival time of a particle at the bottom depends on two unknowns, the starting depth and sinking velocity. Titman (1975) measured the decrease in chlorophyll fluorescence through a 20 mm window at the top of a thermostatted column and verified the method by measurements on uniform coloured beads; the resolution depends on the depth of the window.

In class II, the cell suspension is layered on top of a water column and the descent of the cells is monitored by various means: (i) scanning the base of the column by inverted microscopy (Smayda & Boleyn 1965); (ii) counting cells in samples taken at different depths with a syringe canula (Walsby & Xypolyta 1977; Booker & Walsby 1979); (iii) measuring the cell distribution by

*Author for correspondence (a.e.walsby@bristol.ac.uk).

The electronic supplementary material is available at http://dx.doi.org/10.1098/rsif.2005.0106 or via http://www.journals.royalsoc.ac.uk.

Received 6 October 2005
Accepted 16 November 2005

fluorimetry after a set time by collecting fractions drained from the bottom (Anderson & Sweeney 1977); (iv) observing the change in turbidity or fluorescence as cells arrive at the base of the column (Eppley *et al.* 1967); and (v) observing the depth of a descending cloud of cells (Walsby *et al.* 1983). These methods provide information on average velocities with varying accuracy. Methods (i), (ii) and (iii) provide discontinuous data affected by the intervals of time and depth; (iv) and (v) give data over a range of time with the precision affected by the increasing spread of the distribution. We describe here how quantitative measurements of cell distribution can be made by continuous scanning with a narrow laser beam to reveal the normal distribution of sinking velocities expected for populations of organisms varying over a range of size and orientation.

The laser scanner we describe provides a continuous record of the depth of the sinking cells without perturbing the column. We have verified the method by measuring the sinking velocity of polystyrene microspheres of uniform size and density. Measurements on cyanobacterial filaments also gave velocities that agree with theoretical values based on size, shape and density of the particles. For particles of the size studied (less than 20 μm), the time taken to reach terminal velocity is less than 1 s; for measurements over periods of hours the velocities are, therefore, equal to the terminal velocities. The use of the scanner is applicable to the measurement of sinking in both freshwater and marine systems.

These measurements were made using density gradients that address the two problems afflicting column sedimentation methods. The first is that a simple water column has no stability and tends to circulate: even when thermostatted, the illumination needed for observation causes warming of the layer next to the column wall. The second problem is that the layer of cells applied at the top of the column will have a greater density than the underlying water and will descend *en masse* down the column at a velocity greater than that of individual cells (Walsby 1988). Uniformly increasing the density of the lower layer by adding some denser solution only postpones this because as the cells sink down into the solution they will again form a layer whose density exceeds that of the layer below it. It is, therefore, necessary to prepare a vertically increasing density gradient so that the cells are always sinking into a denser layer (Booker & Walsby 1979).

Density gradients, however, introduce new problems: the sinking rate of the cell progressively decreases as it encounters a solution of increasing density and the associated increasing viscosity. The appropriate correction can be made, though it requires measurement of the cell density (Booker & Walsby 1979). For freshwater forms it is best to use gradients of polymers, such as Ficoll (Conway & Trainer 1972) or Percoll, the substance used here, which has negligible osmotic effects (Walsby *et al.* in press). Sucrose, the substance first employed (Booker & Walsby 1979) is less satisfactory in this respect (Walsby *et al.* in press). For marine and hyposaline phytoplankton, NaCl, which has little viscosity, can be used to provide the density gradient, though the size and buoyant density of the cells may change due to osmosis (Walsby *et al.* 1983). Percoll can be used to make a density gradient in seawater but the results may be compromised by gradual aggregation of the silica sol and interactions with phytoplankton cells (Price *et al.* 1978). We have not investigated Percoll gradients in seawater and the observations made here are limited to freshwater systems.

2. METHODS

2.1. Suspension of particles and cyanobacteria

Monodisperse polystyrene microspheres in 0.29% aqueous suspensions (Duke Scientific, Palo Alto, CA) were of mean diameter 15.02 μm certified to ±0.08 μm with a s.d. of 0.15 μm (traceable size standards, National Institute of Standards and Technology, Gaithersburg, MD) and density 1050 kg m^{-3}. Uniform suspensions of cyanobacterial filaments were obtained from cultures of *Planktothrix rubescens* strain BC *Pla* 9736 (CCAP 1460/11), isolated from Lake Zürich (Beard *et al.* 1999) and grown in the medium of Bright & Walsby (2000).

2.2. Dimensions of the microspheres and filaments

The dimensions of the microspheres were checked by light microscopy using a Leitz Orthoplan light microscope with a ×40 Plan Acromat objective and a Q-imaging digital camera (Micropublisher 5.0 RTV and Q Capture, Quantitative Imaging Corporation). The diameter of each microsphere was determined using an image analysis system (Simple PCI 5.3.1, Compix Inc., Cranberry, PA) calibrated with a stage graticule. The mean diameter of 46 microspheres was 14.98±0.20 μm, in agreement with the certified value, which was used in subsequent calculations. The mean distance between microspheres in the original suspension was equivalent to about 0.1 mm; dispersed in the Percoll solution at the top of the sedimentation column the mean distance between microspheres increased to 0.3 mm, equivalent to 20 microsphere diameters, at the peak of the descending band (§4.1).

The dimensions of *Planktothrix* filaments were determined by microscopy and image analysis. For filament width (w), samples were mounted in the well of a microscope slide with a fixed gap of 10 μm between slide and cover-slip. For filament length (l), samples were collected on 0.22 μm GS filters (Millipore) and imaged by epifluorescence (Walsby & Avery 1996).

2.3. Buoyant density of microspheres and filaments

Density gradient centrifugation (Oliver *et al.* 1981) was used to measure the buoyant density of the microspheres and *Planktothrix* filaments after collapsing gas vesicles by application of 1.4 MPa pressure (Walsby 1971). A linear gradient of Percoll (Sigma), usually from 1% ($\rho = 999.5$ kg m^{-3}) at the top to 95%

($\rho = 1124.4\ \mathrm{kg\ m^{-3}}$) at the bottom, was formed in 15 ml capacity glass centrifuge tubes. The particle suspension was layered over the gradient and the tube was centrifuged for 15 min in a swing-out head of a Coolspin centrifuge (MSE) at 1600 r.p.m., generating an acceleration of $5200\ \mathrm{m\ s^{-2}}$ ($530g$) at the middle of the sample. The microspheres formed an opalescent band and the *Planktothrix* filaments a red band at the isopycnic layer on the gradient; a sample of the band was removed with a fine syringe canula and its refractive index was measured with a refractometer (Bellingham & Stanley, London: No. 935022). The buoyant density of the sample was determined by reference to a refractive-index/buoyant-density calibration curve constructed from measurements on a series of 11 Percoll concentrations.

The mean density of the polystyrene microspheres was determined as $1049.2 \pm 1.2\ \mathrm{kg\ m^{-3}}$, in agreement with the manufacturer's value, $1050\ \mathrm{kg\ m^{-3}}$, which was used in subsequent calculations. The mean densities of the *Planktothrix* filaments are given below (table 2). For marine phytoplankton, which were not investigated here, attention is again drawn to the investigations of Price *et al.* (1978), who describe problems in using Percoll density gradients in seawater.

2.4. Laser scanned sedimentation column

A laser scanner was used to monitor the descent of a population of particles sinking through a vertical density gradient of Percoll in a glass column (figure 1). The column resembles a 100 ml measuring cylinder, but without graduation marks and D-shaped in cross-section, constructed from a cylindrical glass tube (internal diameter 25 mm and height 198 mm) with one side removed and replaced with a flat glass pane cemented in place with epoxy resin.

The column was mounted vertically on a platform that was raised or lowered at a velocity of between 20 and 42 mm $\mathrm{min^{-1}}$ by a motorized worm drive attached to a vertical framework. The worm drive was an engineering screw thread, diameter 8 mm, pitch 1.25 mm; it passed through a screw-threaded hole attached to the platform, which was prevented from rotating by a guide sliding in a channel attached to a vertical support. The motor was a reversible, four-phase stepper motor (RS 440-284, RS Components, Corby Northants, UK) and a 5:1 ratio gear box (RS 718-852) with variable speed settings. Microswitches attached at positions towards the top and base of the framework reversed the direction of the motor when activated by contact with the moving platform; the column could therefore be left unattended, moving up and down past the scanner.

A pen laser (laser diode, wavelength 660–680 nm, maximum output less than 5 mW, with a 3 V direct current voltage-stabilized) was mounted in a fixed position so that, as the sedimentation column was raised, the horizontal beam passed through the centre of the flat pane and the principle axis of the column. Two light signals were collected from the laser beam (figure 2). (i) A small proportion of the incident beam was reflected onto a photodiode from a glass cover-slip,

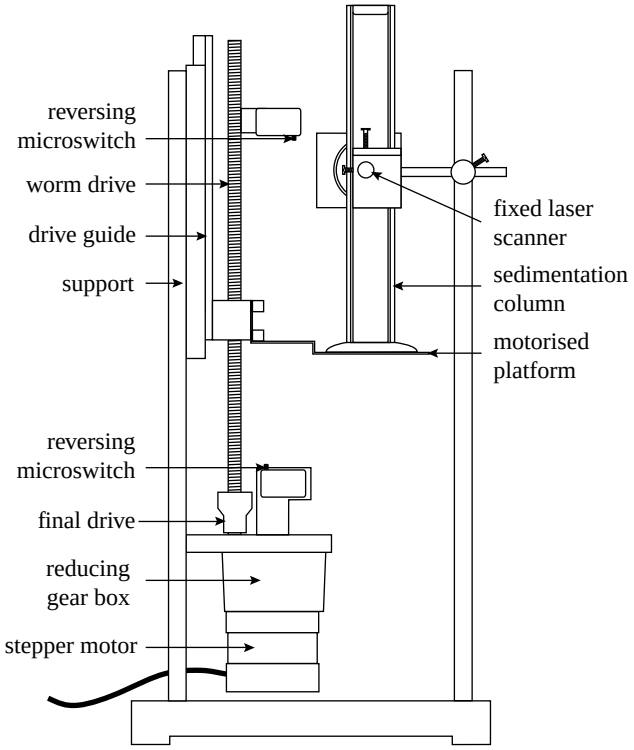

Figure 1. The laser scanner and sedimentation column mounted on a platform raised by a worm drive attached to an electric stepper motor. Microswitches reverse the direction of travel when contacted by the platform. See the moving cartoon in the electronic supplementary material.

held at an angle of about 70° to the beam, on a rotatable mounting between the laser and the column. (ii) Light scattered by particles in the column was collected on a quantum sensor (Macam, SD101Q Cos); the 9 mm wide face of the sensor intercepted forward scattered light at angles between 140 and 160° from the incident beam. The ratio of the two signals provided a correction for variations in laser beam irradiance, used in calculating the proportion of laser light scattered by the particles.

Signals from the photodiode and quantum sensor were collected by a picoammeter (Keithly 485 Autoranging Picoammeter) connected via an analogue-digital interface (HandyScope TiePie) to a PC computer, using HS (HandyScope TiePie) software. The signals were usually recorded at intervals of 1 s (but variable between 0.5 and 300 s). They were saved as .dat files, and analysed in Excel spreadsheets. The relationship between the turbidity signal from the quantum sensor and the concentration of the polystyrene microspheres was investigated by making measurements with a dilution series: the response was linear ($R^2 = 0.992$) up to the maximum concentration tested, which gave a signal of 14 nA. This exceeds the maximum signal (9 nA) in the scans reported below.

Conceptually, it would be preferable to keep the column stationary and to move the scanning device: in practice it proved difficult to maintain the precise horizontal alignment of the scanning device when it was moved vertically, owing to its greater mass, width and the encumbrance of the photocell wiring.

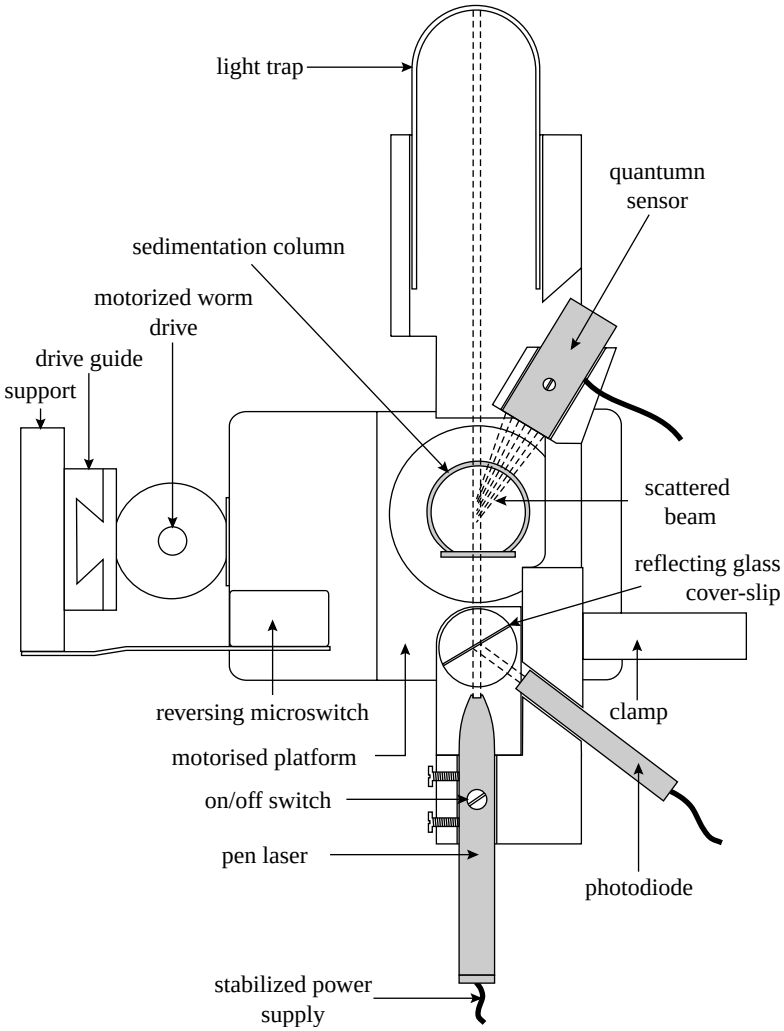

Figure 2. Plan view of the scanner showing light path of the laser beam (dashed lines) in relation to the sedimentation column (shown in cross-section). Part of the incident beam is reflected to a photodiode. Forward-scattered light from suspended particles is collected by a quantum sensor, located at 150° to the incident beam.

2.5. Water column stabilized by a Percoll density gradient

The sedimentation column was usually filled to a depth of 150 mm (within 50 mm of the top) with a suspension of Percoll forming a linear gradient of concentration, usually from 1% ($\rho = 999.5\ \mathrm{kg\ m^{-3}}$) at the top to 15% ($\rho = 1018.2\ \mathrm{kg\ m^{-3}}$) at the bottom, by the standard two-cylinder method: Percoll solutions of low and high density are placed in two identical, joined cylinders; as the contents of the first cylinder drain into the bottom of the sedimentation column, the contents of the second drain into the first and are mixed there, giving a linear concentration increase in the column (Bock & Ling 1954). The Percoll concentration at the top was chosen to give a density that was higher than the density of the suspension of the particles (but less than the density of the particles themselves), so that the suspension floated on the gradient; the Percoll concentration at the bottom was also less than that of the particles, so that the particles did not stop sinking on reaching an isopycnic layer before the bottom.

The column was placed on the platform of the scanner, which was adjusted to scan repeatedly from a position 37 mm above the liquid to 114 mm below the surface, the 151 mm total taking 220 s (i.e. at $0.69\ \mathrm{mm\ s^{-1}}$). After leaving the column to stabilize for a few hours trial scans with the laser were made to check that the column was aligned and free of optical perturbations, giving a smooth baseline. A small volume of the suspension was slowly pipetted onto the column and the column was left to scan continuously for several hours.

2.6. Analysis of turbidity profiles

2.6.1. Distribution of particle sinking velocities. The data from each scan comprises a series of turbidity measurements at 1 s time intervals. The depth at each measurement was calculated from the scan speed and by reference to a signal from the beam defracted at the meniscus at the top of the column. The corresponding depth to which a particle would have sunk in water was calculated with the corrections for density and viscosity of the Percoll gradient given in §3.3. The distribution of sinking velocities in water was calculated in Excel spreadsheets from the turbidity and the corrected depth of each measurement. Measurements on sinking microspheres gave distributions of sinking velocities that closely resembled normal distributions, in which

the mean turbidity coincided with the maximum turbidity (§4.1).

2.6.2. Synoptic correction for graphical display. Because the primary data is obtained at successive time intervals and not depths *per se*, graphical representation of the turbidity distribution with depth requires a correction for the time change during each scan. Each laser scan starts at the fixed reference point, z_f, above the column determined by the position of the reversing switch (figure 1); the scanner passes down through z_0, the meniscus at the top of the gradient (recorded as a dip in the turbidity reading) and it reverses at a depth z_s just above the bottom of the column, returning to z_f. The time for one scan is t_s, which includes the period t_m between z_f and z_0; for N upward and downward scans the time is t_sN. Suppose that as the scanner returns to z_0 after N scans, a particle has reached a depth z_c; the scanner will next intercept the particle at the slightly greater depth z_a and the later time t_a. The mean velocity of the particle over the period of N scans is therefore approximately $z_a/(t_sN + t_a)$ and the depth of the particle at the start of the Nth scan is approximately

$$z_c = z_a t_s N/(t_a + t_s N). \tag{2.1}$$

For graphical representation of turbidity with depth (rather than time) this depth correction is applied to each 1 s time interval in each downward scan. For an upward scan the corrected depth is

$$z_c = z_a(t_s N - t_m)/[t_s(N+1) - 2t_m - t_a]. \tag{2.2}$$

For the microspheres and cyanobacteria described, whose sinking velocities are about 0.01 of the scanning speed, the difference between z_a and z_c is only 0.75% when the particles have sunk 0.37 of the depth of the column. The precise difference, calculated from the distribution of sinking velocities rather than the distribution of depths, is 0.67%.

3. THEORY OF SINKING VELOCITY AND CORRECTIONS NEEDED

Cultures and samples of natural phytoplankton contain cells at different stages of the cell cycle that differ in shape, size and density: all of these factors affect the sinking velocity, which therefore varies. Measurements, therefore, require determination of the mean velocity and the distribution of velocities.

3.1. The sinking velocity of a particle

For a sphere sinking in water the velocity expected is given by the Stokes equation

$$u = 2gr^2(\rho' - \rho)/9\eta, \tag{3.1}$$

where g is the gravitational acceleration (9.81 m s^{-2}), r is the sphere's radius, ρ' is its density, ρ is the density of the water, and η its coefficient of dynamic viscosity. For the microspheres of $r = 7.51$ µm, $\rho' = 1050.0$ kg m^{-3} sinking in water of density $\rho = 998.2$ kg m^{-3} and viscosity $\eta = 1.0019\times10^{-3}$ kg m^{-1} s^{-1} at 20 °C, the calculated velocity is $u = 6.36$ µm s^{-1}. The Stokes equation holds when the viscous forces exceed the inertial forces, indicated by a Reynolds number, Re, less than unity:

$$Re = 2ru\rho/\eta. \tag{3.2}$$

Substituting the same values gives $Re = 9.5\times10^{-5}$, well within the Stokes range. This theoretical value can, therefore, be compared with the observed sinking velocity, $u = z/t$, where z is the depth that the sphere sinks in time t.

For other shapes an additional factor is applied, the coefficient of form resistance, ϕ. For non-spherical particles of regular shape, values of ϕ are calculated for ellipsoids of similar axial ratios (see below); the effective radius r_e is calculated as that of the sphere of identical volume, $r_e = (3V/4\pi)^{1/3}$, and the sinking velocity in water is then

$$u = 2gr_e^2(\rho' - \rho)/9\eta\phi. \tag{3.3}$$

3.2. Sinking rates and form resistance of cylindrical filaments

McNown & Malaika (1950) showed that non-spherical objects remain in their original orientations when sinking at low Reynolds numbers as long as they are symmetrically weighted. (The familiar re-orientation towards maximum resistance, e.g. coins falling in a bucket of water, occurs at higher Reynolds numbers, when flow is not laminar). There is no exact theory for the sinking rate of a cylinder but McNown & Malaika (1950) showed experimentally that, at low Reynolds numbers, the settling velocity of a cylindrical object was similar to that of an ellipsoid of the same axial ratio, volume and density. They provided equations for the form resistance, ϕ, for an ellipsoid:

$$\phi = 16/[3D(\alpha + \beta)], \tag{3.4}$$

in which α is a shape factor independent of orientation, β is a shape factor that depends on orientation relative to the direction of movement, and D is the nominal diameter. For an ellipsoid (with semi-axes a, b and c)

$$D = 2(a\ b\ c)^{1/3}. \tag{3.5}$$

In the two cases in which the principal axis is either vertical or horizontal, a is the vertical axis, while both b and c are in the horizontal plane. For the ellipsoid of the same axial ratio as the cylindrical filament, when the principal axis is vertical, $a > b = c$ and then

$$\alpha = \{2/[(a^2 - c^2)^{0.5}]\}\{\tanh^{-1}[(a^2 - c^2)^{0.5}/a]\}, \tag{3.6}$$

$$\beta = \{2a^2/[(a^2 - c^2)^{1.5}]\}\{\tanh^{-1}[(a^2 - c^2)^{0.5}/a] - [(a^2 - c^2)^{0.5}/a]\}. \tag{3.7}$$

When the same ellipsoid is falling with the principal axis horizontal, $a = c < b$ and

$$\alpha = \{2/[(b^2 - a^2)^{0.5}]\}\{\tanh^{-1}[(b^2 - a^2)^{0.5}/b]\}, \tag{3.8}$$

$$\beta = \{a^2/[(b^2 - a^2)^{1.5}]\}\{[b(b^2 - a^2)^{0.5}/a^2] - \tanh^{-1}[(b^2 - a^2)^{0.5}/b]\}. \tag{3.9}$$

For a given ellipsoid, oriented either vertically or horizontally, substitution of α and β in equation (3.4)

gives the minimum and maximum values of form resistance, ϕ_v and ϕ_h, respectively.

The filaments of *P. rubescens* are cylinders of width w, length l and volume $V_c = \pi(w/2)^2\, l$. For a filament oriented vertically, the form resistance ϕ_v is calculated by putting $l/2 = a$, and $w/2 = b$ and c in equations (3.6) and (3.7) to obtain the values of α and β in equation (3.4); its sinking velocity (u_v) is then given by putting $\phi_v = \phi$ and $(3\,V_c/4\pi)^{1/3} = r_e$ in equation (3.3). A similar procedure is used for the sinking velocity of the horizontally oriented filament (u_h), except that ϕ_h is calculated by putting $l/2 = b$, and $w/2 = a$ and c in equations (3.8) and (3.9).

3.3. The density-viscosity correction for Percoll

For a sphere sinking down a column stabilized by a concentration gradient, the velocity is affected by the increasing density and viscosity. On a linear concentration gradient ($B = \mathrm{d}C/\mathrm{d}y$) the concentration ($C$) at depth y is given by $C = A + By$, where A is the concentration at the top of the column. Assuming that the viscosity and density vary linearly with concentration (which is true for Percoll at low concentrations) then at depth y the density $\rho_y = \rho_0(1 + \tau C)$ and the viscosity $\eta_y = \eta_0(1 + \varphi C)$, where τ is the coefficient of relative density change per concentration (units of $\%^{-1}$) and φ is the coefficient of relative viscosity change per concentration (also in units of $\%^{-1}$); ρ_0 and η_0 are the density and viscosity at zero concentration (i.e. of water). If in a given time, t, a particle sinks down the gradient to a depth y, the depth to which it would sink in water, y_0, can be calculated by using the Rothschild–Simpson equation (Booker & Walsby 1979):

$$y_0 = [(\rho' - \rho_0)/(\rho_0 B\tau)]\{[1 + \varphi(\rho' - \rho_0)/\rho_0\tau] \times \ln[(\rho' - \rho_0(1 + \tau A))/(\rho' - \rho_0(1 + \tau A + \tau By))] - \varphi By\}. \quad (3.10)$$

For Percoll, $\tau = 0.00133\%^{-1}$; $\varphi = 0.02037\%^{-1}$. The values of A and B vary: in the gradient described below for microspheres, $A = 1.22\%$ (w/v); $B = 95.5\%$ (w/v) m^{-1}. A 100% concentration Percoll (Sigma) colloidal solution (of osmolality less than 20 nOsm kg^{-3}, and pH 8.9 ± 0.3 at 20 °C) has a density at 20 °C of 1130 kg m^{-3} and a viscosity of 10 ± 5 cp. The excess density of the full strength solution is, therefore, $1130 - 998.2 = 131.8$ kg m^{-3}. For a solution of Percoll in water with a density $\rho = 1020$ kg m^{-3} (i.e. an excess density of 22 kg m^{-3} (Walsby *et al.* in press), which is 22 kg m^{-3}/132 kg $\mathrm{m}^{-3} = 1/6$ full strength), the viscosity was 1.365×10^{-3} kg m^{-1} s^{-1}: for the original full strength solution the expected viscosity is, therefore, 1.365×10^{-3} kg m^{-1} $\mathrm{s}^{-1} \times 6 = 8.2 \times 10^{-3}$ kg m^{-1} s^{-1} (within the manufacturer's range, $(10 \pm 5) \times 10^{-3}$ kg m^{-1} s^{-1}). An Excel spreadsheet for calculating the density-viscosity correction, equation (3.10), is available in the electronic supplementary material.

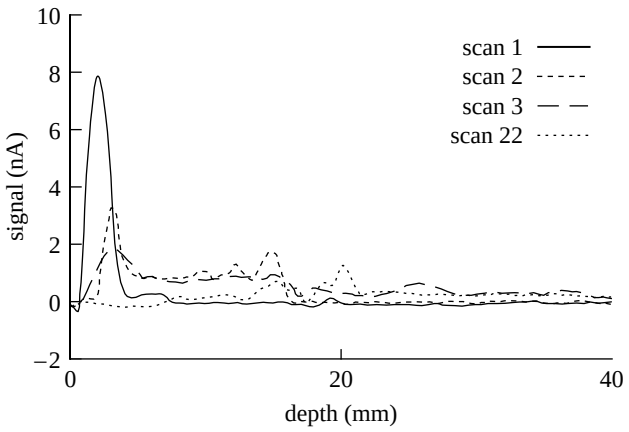

Figure 3. The time course of microspheres sedimenting down a uniform Percoll column, showing laser scans 1, 2, 3 and 22 (starting after 0, 220, 440 s and 77 min).

4. RESULTS

4.1. Sedimentation of polystyrene microspheres

Two drops of the microsphere suspension were added at the top of the Percoll solution prepared in some cases as a uniform 1.5% solution and in others as a 1–15% gradient in the sedimentation column. The microspheres entered the Percoll column where at first they formed a sharply defined turbid layer. The behaviour of this layer was very different in the uniform and gradient columns.

4.1.1. Sedimentation through a uniform Percoll solution. The sharply defined turbid layer first showed clearly as a normal curve with a maximum at a depth of 2 mm in the first downward scan (figure 3); by the second, upward, scan, begun 220 s later, the corresponding curve, at a similar depth, had become flattened with a peak height of only 42% of the previous value; below it was a raised baseline with a cluster of smaller peaks at a depths of 10, 12 and 15 mm. The velocity inferred from the depth of the third and largest minor peak was 13 mm/220 s = 59 μm s^{-1}, which is nine times faster than expected from the Stokes equation. This suggests that part of the initial microsphere band became detached from the unstable surface layer and descended as a drop, trailing microspheres through the uniform Percoll solution. In the third scan, the surface peak was further flattened and there were additional losses to minor peaks descending below. After 22 scans there were two main peaks whose heights were only 9 and 16% of the initial value at depths of 15 and 20 mm, respectively (figure 3); this indicated sinking velocities of 2.8 and 3.9 μm s^{-1}, rather less than the expected value. In summary, the unstable nature of the uniform Percoll column resulted in density induced convection currents that accelerated the vertical movement of some microspheres and delayed the sinking of others.

These irregularities were seen in further experiments, though the details varied. In one such experiment in which the bead suspension was layered over a higher (uniform) concentration of Percoll, 7%,

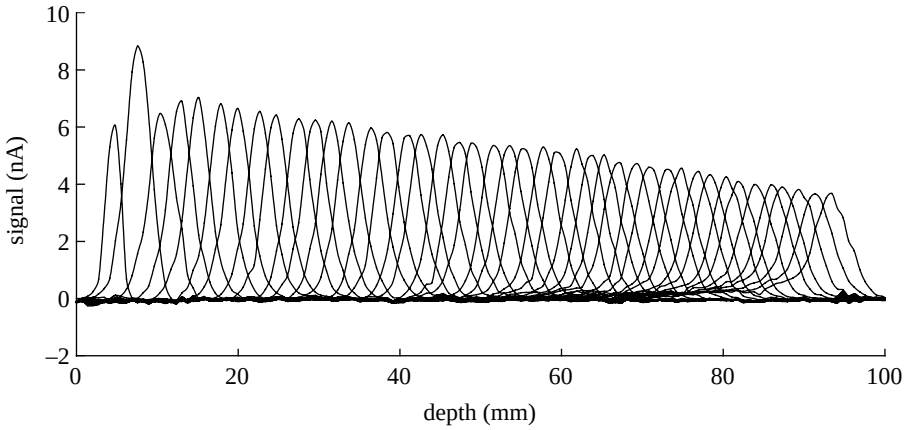

Figure 4. The time course of sedimentation by a band of microspheres down the Percoll gradient, showing the 43 downward scans of the 86 scans by the laser.

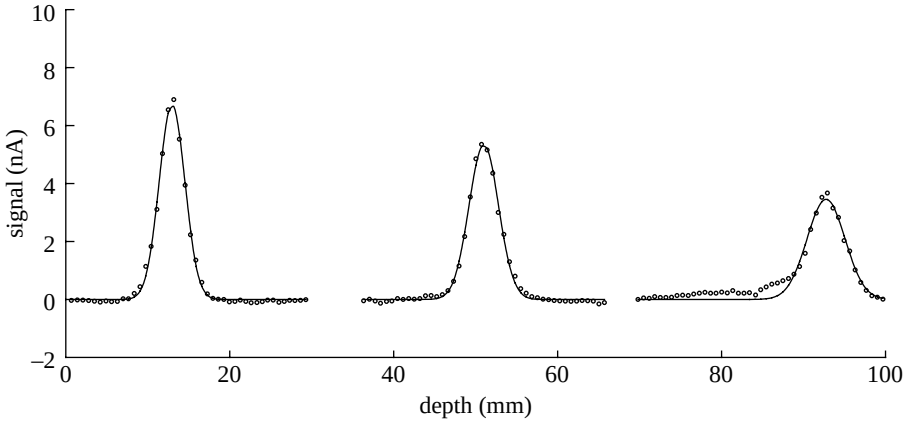

Figure 5. Measurements of microsphere concentration at different depths indicated by scans with the laser. The markers indicate measurements made at 1 s intervals during scans 7, 41 and 85 (starting after 22, 147 and 308 min), corrected for differences in measurement time. The continuous lines show the normal distributions most closely resembling the measured distributions.

this did not improve the stability of the system: clusters of beads sank at even higher velocities, up to 380 μm s^{-1}, 60 times faster than the Stokes value.

4.1.2. Sedimentation through a Percoll gradient. The Percoll gradient evidently provided stable conditions for observing the sinking particles over long periods: sharply defined turbid layers were found in 86 consecutive scans made over 5.2 h (figure 4). In each successive scan, the depth of the turbidity maximum increased by about 1 mm; the initial change in depth of the maximum indicated a mean sinking velocity of about 6 μm s^{-1} (similar to the Stokes value in water) and falling below 4 μm s^{-1} towards the end. As shown below, applying corrections for the increasing viscosity and density of the Percoll solution gave a velocity in water very close to that calculated by the Stokes equation.

Each of the 86 turbidity profiles of the successive scans was normally distributed. After the first five scans, the observed distributions showed a small progressive decrease in peak height (by an average of 0.6% between adjacent scans) and a corresponding increase in width (also 0.6%); the uniformity of the decrease in peak height suggested the gradual diffusion of the descending band (figure 4). The variation in the first few turbidity profiles is attributed partly to uneven mixing of the microsphere suspension added to the top of the Percoll column, and partly to optical distortion of the laser beam near the meniscus at the top of the column. We, therefore, take as a starting reference point the maximum of the turbidity profile in scan number 6.

Details of turbidity profiles recorded in three downward scans, numbers 7, 41 and 85 shown in figure 5, are used to determine the proportion of microspheres detected within the sinking turbidity bands after different times. In each case, the markers in figure 5 indicate the turbidity measurements made at 1 s time intervals. These data have been corrected using equations (2.1) and (2.2) to give curves synoptic with the first reading at the start of each scan. The lines represent normal distributions most closely resembling the observed distributions. The relative proportions of the microspheres recorded in each scan, calculated as the integral of readings under each measured turbidity curve, were 1.00, 0.932 and 0.898; this indicates a loss of only 10.2% over the 78 scans or 0.13% between adjacent scans. Most of the microspheres remained in a coherent band, though in the later scans a small proportion of the turbidity was left in a tail above the descending peak.

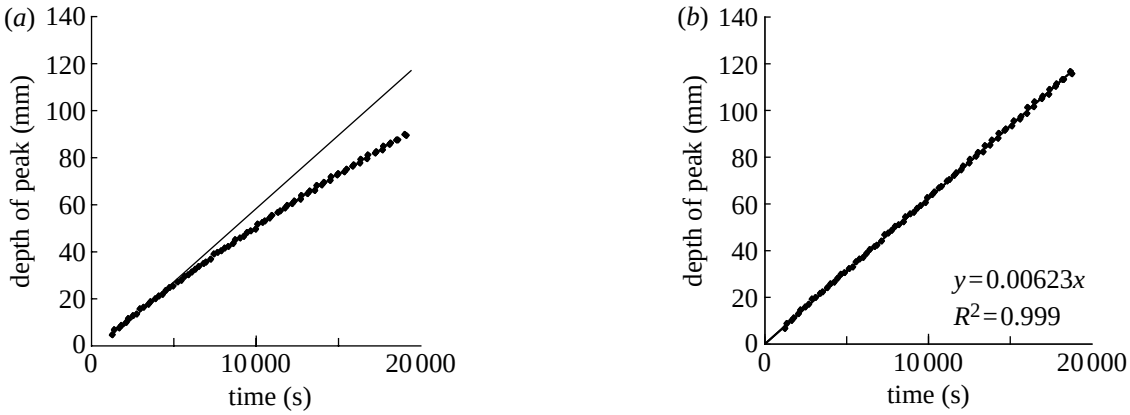

Figure 6. The change in depth of the turbidity maximum of the sinking microsphere band with time: (*a*) measured values in the Percoll gradient; (*b*) the values calculated for the microspheres sinking in water at 20 °C, corrected for differences in viscosity and density of the Percoll gradient. The line in (*a*) is the regression line of the data in (*b*).

The mean sinking velocity of the microspheres was determined by analysis of the change in depth of the turbidity maximum with time in scans 6–86 (figure 6*a*). The depth of the maximum steadily increased with time, but in a curvilinear fashion: the sinking velocity gradually decreased as the microspheres sank into layers of increasing density and viscosity.

The effects of these two factors in decreasing the sinking velocity were determined from the change in Percoll concentration (B) using equation (3.10): from the measured depth of the maximum in each scan (y) at each time (t), the equivalent depth to which the microspheres would have sunk in water (y_0) was calculated. The depths of the turbidity maximum corrected in this way show a precisely linear increase with time (figure 6*b*). The gradient of the depth/time line indicated the equivalent sinking velocity in water at 20 °C, 6.23 μm s^{-1}, very close to that calculated by the Stokes equation for spheres of the same density and volume as the microspheres, 6.36 μm s^{-1}. Three further measurements of sinking velocity made with new microsphere samples on replica Percoll gradients yielded similar values (table 1): the mean of the four velocities, 6.28 μm s^{-1}, differed by only 1.3% from the Stokes value.

The width of the band of descending microspheres remained remarkably tight over the period of observations (figures 4 and 5). Such broadening that did occur in the turbidity curve has several possible causes: variation in the sinking velocities owing to variations in size and density; inhomogeneities in the distribution of Percoll particles; thermal diffusion; viscous drag on the particles at the walls of the sedimentation column. McNown & Malaika (1950) showed that the correction for drag on a single particle of diameter D sinking in a column of diameter D_c is given by

$$K = 1 + (9D/4D_c) + (9D/4D_c)^2. \qquad (4.1)$$

For the microspheres ($D = 15$ μm) settling in the sedimentation column ($D_c = 25$ mm), K has a value of 1.0014. Nevertheless, particles close to the walls may experience significant drag and this may be the main cause of the tail above the descending band.

Table 1. Comparison of the sinking velocities of standard microspheres measured with the scanner (u_0) and calculated by the Stokes equation (u_s).

run	measured u_0 (μm s^{-1})	calculated u_s (μm s^{-1})	ratio u_0/u_s
1	6.23	6.36	0.98
2	6.26	6.36	0.98
3	6.23	6.36	0.98
4	6.38	6.36	1.00
mean			0.99±0.01

4.2. Sedimentation of filaments of P. rubescens

Measurements were made with the scanner of the sinking velocities of several species of freshwater phytoplankton on Percoll density gradients. Spherical phytoplankton cells, such as those of the green alga *Chlorella* sp. and the cyanobacterium *Microcystis* sp., which form even suspensions, produced well-defined sinking bands, though with a wider distribution than the microspheres owing to the range of size and density (Walsby *et al.* in press). A more severe test of the method was provided by measurements on filamentous organisms, in which the velocity is affected by not only the natural variation in density and size but also the orientation of the filaments.

The sinking velocity of the filamentous cyanobacterium *P. rubescens*, which forms well-dispersed suspensions, was investigated using a Percoll gradient made in the same way as that used above (figure 7*a*). Every 10th scan (fifth downward scan) is shown in figure 7*a*. The turbidity profiles showed broader distributions and more noise than those of the uniform spheres. The broader initial distribution indicates a greater variation in sinking velocity, which is expected for two reasons: the filaments vary in length, which affects r_e (§3.1) and ϕ (§3.2); the filaments vary in orientation, which affects the shape factor β, a component of ϕ (§3.2). It follows that the variation in depth distribution will increase with time as the slower filaments lag behind the faster.

Despite the noise, a plot of the depth of the turbidity maximum against time (for the first 46 scans),

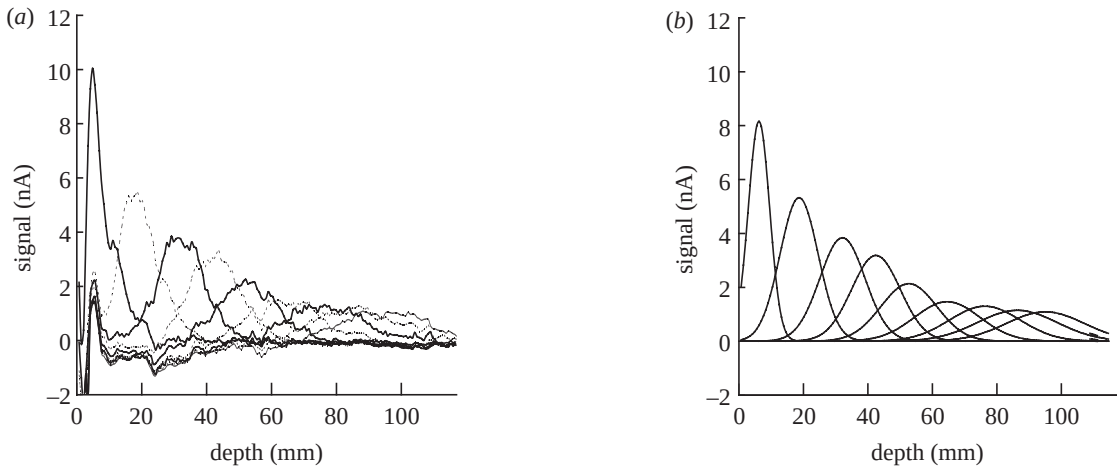

Figure 7. The time course of sedimentation by a suspension of *Planktothrix* filaments down the Percoll gradient revealed by scans with the laser. (*a*) Measured turbidity distributions in every tenth scan (fifth downward scan), alternately with broken and continuous lines. (*b*) Normal distributions most closely resembling the measured distributions.

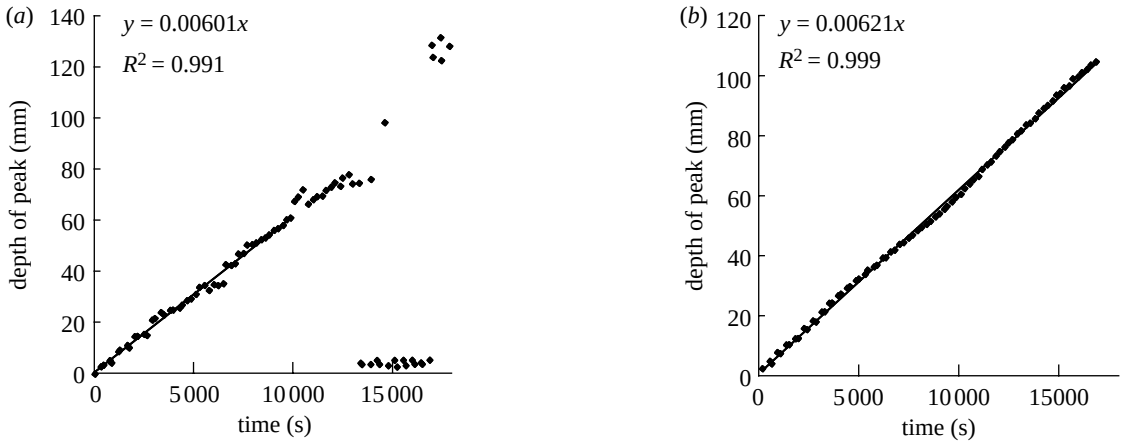

Figure 8. The change in equivalent depth of the maximum *Planktothrix* concentration with time in each scan: (*a*) depth of the maxima of the measured turbidities in each of the 84 scans, and the regression line for the first 46 scans; (*b*) depth of the maxima of the normal distributions most closely resembling the measured distributions for the 84 scans and the regression line through the full range. Depths shown are the equivalent depths for sinking in water at 20 °C, after correction for differences in viscosity and density of the Percoll gradient.

Table 2. Comparison of the sinking velocities of *Planktothrix* filaments measured with the scanner (u_0) and calculated by the Stokes equation with form resistance corrections: u_v, with filament vertical; u_h, filament horizontal; u_m the mean of u_v and u_h.

run	density (kg m^{-3})	mean width (μm)	mean length (μm)	u_0 (μm s^{-1})	u_v (μm s^{-1})	u_h (μm s^{-1})	u_m (μm s^{-1})	ratio u_0/u_m
1	1092	4.52	174	6.21	7.19	4.61	5.90	1.05
2	1085	4.50	164	5.46	6.61	4.24	5.42	1.01
3	1084	4.50	173	6.14	6.30	4.06	5.18	1.19
mean								1.08±0.09

corrected for the increasing viscosity and density of Percoll, showed a linear increase with time, with an R^2 of 0.991 (figure 8*a*). The slope of depth versus time indicated a sinking velocity of 6.01 μm s^{-1}. Noise in the turbidity signal generated errors in the mean depth of the turbidity distribution and especially in the later, flatter distributions. A better estimate of the mean depth of the *Planktothrix* distribution was obtained from the mean of the normal distribution that most closely resembled the measured turbidity distribution in each scan. The normalized distributions are shown in figure 7*b* and the depths of the normalized maxima for the full 84 scans are shown in figure 8*b*. It is seen that the plot is linear ($R^2 = 0.999$) over the full range and the scatter is less than that of the measured maxima. The gradient over the first 46 scans indicates a velocity of 5.90 μm s^{-1}, similar to that based on the turbidity maxima; that over the full range of 84 scans gives a slightly higher velocity, 6.21 μm s^{-1}. Some details of the distribution of sinking rates are lost in the process of

normalization but an improved estimate is obtained of the mean velocity when there is a low ratio of signal to noise.

4.3. Comparison of observed and expected velocities

The buoyant density of the filaments in the *Planktothrix* sample (used in figures 7 and 8) was determined by isopycnic centrifugation to be 1091.6 kg m^{-3}. Measurements made by microscopy of the filaments in the same sample indicated a mean width of 4.52 ± 0.15 μm ($n = 14$) and a mean length of 174 ± 148 μm ($n = 101$). The sinking velocities in water were calculated individually for each of the 101 measured values of filament length, assuming the same mean width and density: the mean values for the population were, for the maximum (u_v) 7.19 μm s^{-1}, and the minimum (u_h) 4.61 μm s^{-1}. The observed value, 6.21 μm s^{-1}, is close to the average of these two extremes, 5.90 μm s^{-1}; similar agreement was found in the measurements made on two other *Planktothrix* samples (table 2). For a sample of filaments oriented uniformly over all angles in three dimensions, however, the proportion at an angle θ to the horizontal will vary as $\cos\theta$. Dr J. C. Gill provided the following solution for the average of angle θ:

$$\theta_m = \left(\int_0^{\pi/2} \theta \cos\theta \, d\theta\right) \Big/ \left(\int_0^{\pi/2} \cos\theta \, d\theta\right)$$

$$= (\pi/2 - 1)/1 = 0.571 \text{ rad}. \quad (4.2)$$

This mean value, 32.7°, is less than the arithmetic mean of 45° between 0 and 90° and it may be expected that the mean velocity will be closer to u_h than to u_v. Although, analytical solutions exist for the sinking velocity of ellipsoids oriented at angles of 0 and 90° to the horizontal, none are available for the intermediate angles; it is therefore not possible to make more precise statements about the mean velocity expected for forms that are oriented randomly or uniformly.

While objects that are symmetrically weighted remain in their original orientations when sinking at low Reynolds numbers, those that are asymmetrically weighted will sink heavy-end down (McNown & Malaika 1950). The *Planktothrix* filaments investigated here are symmetrically shaped but it is inevitable that a proportion of them will be asymmetrically weighted and will tend to become reoriented with their long axes vertical. This may explain why the mean of their measured sinking velocities slightly exceeded u_m.

5. DISCUSSION

The combination of the scanner and Percoll gradient provides perhaps the most precise measurements that have been made of the sinking rates of phytoplankton-size particles. Verification of the Stokes equation has previously entailed experiments with larger spheres sinking in tanks of more viscous fluids to give low Reynolds numbers (McNown & Malaika 1950).

The scanner itself is easy to operate and can be left operating unattended. The main difficulties in obtaining accurate measurements of sinking velocities in water are those involved in the additional measurements of the size (by microscopy) and buoyant density (by isopycnic centrifugation) of the sinking particles, though these measurements may be needed for other purposes. If they are not, a useful calculation of the velocity can be obtained by the initial slope of depth/time when the particles are sinking through the layers of lowest concentration (figure 6*a*).

It appears from the past literature that the measurement of sinking velocities of small particles is regarded as a simple task requiring little sophistication. The scanned gradient provides a standard against which other methods can now be compared. The comparison made here shows how essential it is to stabilize the sedimentation column. Apart from verifying other published methods, however, the new method can be used in the investigation of factors affecting the suspension of planktonic organisms, including the following: the difference in sinking rate of living and dead cells; discrepancies between theoretical and measured sinking velocities of different phytoplankton species; the effect on cell form resistance of various protuberances on cells, such as the bristles on *Scenedesmus*, and the chitin fibres of *Thalassiosira*; the effects of complex shapes on form resistance of cells or colonies, e.g. the asterisk-like *Asterionella*.

A restriction in the use of the scanner is that it will not distinguish cells of different types or species, for example, in samples from natural populations. The column density gradient, based on Percoll mixtures, is universally applicable, however, and could be used with advantage in combination with other methods that will distinguish different cell types. The scanner and gradient can also be used to measure the floating velocity of buoyant cells, such as certain marine diatoms and gas-vacuolate cyanobacteria, which, when introduced at the base of the column in a concentrated solution of Percoll, will float up into the overlying gradient (Walsby *et al.* 1983).

The method described here is applicable to both freshwater and marine phytoplankton but for the latter, substances other than Percoll may be needed. Price *et al.* (1978), who investigated several substances for the separation of different marine phytoplankton species by density gradient centrifugation, found Percoll was better than other polymers: cells remained active and viable in Percoll and the sol formed stable mixtures with sea water. Over prolonged periods (several days), however, an increase in turbidity indicated aggregation of the silica sol. While Percoll may be satisfactory for stabilizing the sedimentation columns over short periods, it appears to be less satisfactory for determining the density of marine phytoplankton, as the density of some phytoplankton cells exceeds the maximum density of Percoll. Price *et al.* (1978) added sorbitol, which permitted isopycnic banding of the cells, but the osmotic effects of the sorbitol would cause changes in cell volume and density. Price *et al.* (1978) also drew attention to the possibility that the densities of cells might be altered in the presence of polymers and by changes in pH, so that the banding density might not correspond to their true

density. We found no discrepancy between the density of the polystyrene microspheres and their banding density on centrifuged Percoll gradients. Nevertheless, there are potential errors here that should be checked by an independent method of density determination.

We thank Linda Tiegle for constructing the stepper motor controls and Paul Chappell for machining the scanner housing and drive of the laser scanned column, and Tim Colborn for creating the moving cartoon of the equipment. Preliminary studies on Percoll gradients were made by Patricia Lihou and Juliet Roper and on the scanner by Phillip Davis. We thank Colin Gill who kindly provided equation (4.2). This study was supported by a grant to AEW from the NERC and a Overseas Research Studentship from Universities UK to DPH.

REFERENCES

Anderson, L. W. & Sweeney, B. M. 1977 Diel changes in the sedimentation characteristics of *Ditylum brightwelli*: changes in cellular lipid and effects of respiratory inhibitors and ion-transport modifiers. *Limnol. Oceanogr.* **22**, 539–552.

Beard, S. J., Handley, B. A., Hayes, P. K. & Walsby, A. E. 1999 The diversity of gas vesicle genes in *Planktothrix rubescens* from Lake Zürich. *Microbiology* **145**, 2757–2768.

Bienfang, P. K. 1981*a* Sinking rates of heterogeneous, temperate phytoplankton populations. *J. Plankton Res.* **3**, 235–253.

Bienfang, P. K. 1981*b* A technologically simple and reliable method for measuring phytoplankton sinking rates. *Can. J. Fish. Aquat. Sci.* **38**, 1289–1294.

Bock, R. M. & Ling, N.-S. 1954 Devices for gradient elution chromatography. *Anal. Chem.* **26**, 1543–1546. (doi:10.1021/ac60094a004)

Booker, M. J. & Walsby, A. E. 1979 The relative form resistance of straight and helical blue-green algal filaments. *Br. Phycol. J.* **14**, 141–150.

Bright, D. & Walsby, A. E. 2000 The daily integral of growth by *Planktothrix rubescens* calculated from growth rate in culture and irradiance in Lake Zürich. *New Phytol.* **146**, 301–316. (doi:10.1046/j.1469-8137.2000.00640.x)

Conway, K. & Trainor, F. R. 1972 *Scenedesmus* morphology and flotation. *J. Phycol.* **8**, 138–143.

Eppley, R. W., Holmes, R. W. & Strickland, J. D. H. 1967 Sinking rate of marine phytoplankton measured with a fluorimeter. *J. Exp. Mar. Bio. Ecol.* **1**, 191–208. (doi:10.1016/0022-0981(67)90014-7)

McNown, J. S. & Malaika, J. 1950 Effect of particle shape on settling velocity at low Reynolds numbers. *Trans. Am. Geophys. Un.* **31**, 74–82.

Oliver, R. L., Kinnear, A. J. & Ganf, G. G. 1981 Measurements of cell density of three freshwater phytoplankters by density gradient centrifugation. *Limnol. Oceanogr.* **26**, 285–294.

Price, C. A., Reardon, E. M. & Guillard, R. R. L. 1978 Collection of dinoflagellates and other marine microalgae by centrifugation in density gradients of a modified silica sol. *Limnol. Oceanogr.* **23**, 548–553.

Smayda, T. J. 1970 The suspension and sinking of phytoplankton in the sea. *Oceanog. Mar. Biol.* **8**, 353–414.

Smayda, T. J. 1971 Normal and accelerated sinking of phytoplankton in the sea. *Mar. Geol.* **11**, 105–122. (doi:10.1016/0025-3227(71)90070-3)

Smayda, T. J. 1974 Some experiments on the sinking characteristics of two freshwater diatoms. *Limnol. Oceanogr.* **19**, 628–635.

Smayda, T. J. & Boleyn, B. J. 1965 Experimental observations on the flotation of marine diatoms. I. *Thalassiosira* cf. nana, *Thalassiosira rotula* and *Nitzschia seriata*. *Limnol. Oceanogr.* **10**, 499–509.

Titman, D. 1975 A fluorometric technique for measuring sinking rates of freshwater phytoplankton. *Limnol. Oceanogr.* **20**, 869–875.

Waite, A. M. & Nodder, S. D. 2001 The effect of *in situ* iron addition on the sinking rates and export flux of Southern Ocean diatoms. *Deep-Sea Res. II* **48**, 2635–2654. (doi:10.1016/S0967-0645(01)00012-1)

Walsby, A. E. 1971 The pressure relationships of gas vacuoles. *Proc. R. Soc. B* **178**, 301–326.

Walsby, A. E. 1988 Buoyancy in relation to the ecology of the freshwater phytoplankton. In *Algae and the aquatic environment* (ed. F. E. Round), pp. 125–137. Bristol: Biopress Ltd.

Walsby, A. E. & Avery, A. 1996 Measurement of filamentous cyanobacteria by image analysis. *J. Microbiol. Meth.* **26**, 11–20. (doi:10.1016/0167-7012(96)00816-0)

Walsby, A. E. & Reynolds, C. S. 1981 Sinking and floating. In *The physiological ecology of phytoplankton* (ed. I. Morris), pp. 371–412. Oxford: Blackwell Scientific Publications.

Walsby, A. E. & Xypolyta, A. 1977 The form resistance of chitan fibres attached to the cells of *Thalassiosira fluviatilis* Hustedt. *Brit. Phycol. J.* **12**, 215–223.

Walsby, A. E., Van Rijn, J. & Cohen, Y. 1983 The biology of a new gas-vacuolate cyanobacterium, *Dactylococcopsis salina* sp. nov., in Solar Lake. *Proc. R. Soc. B* **217**, 417–447.

Walsby, A. E., Lihou, P. & Roper, J. In press Variation in sinking velocity and cell size of *Microcystis* sp. *Arch. Hydrobiol. Suppl, Algolog. Stud.*

Wiseman, S. W. & Reynolds, C. S. 1981 Sinking rate and electrophoretic mobility of the freshwater diatom *Asterionella formosa*: an experimental investigation. *Br. Phycol. J.* **16**, 357–361.